Research article

Journal of PeptideScience

Received: 24 April 2015 Revised: 8 August 2015 Accepted: 3 September 2015 Published online in Wiley Online Library

(wileyonlinelibrary.com) DOI 10.1002/psc.2826

Effect of distal sugar and interglycosidic linkage of disaccharides on the activity of proline rich antimicrobial glycopeptides

Deepti S. Lele,† Rohini Dwivedi,† Saroj Kumari and Kanwal J. Kaur*

The effect of glycosylation on protein structure and function depends on a variety of intrinsic factors including glycan chain length. We have analyzed the effect of distal sugar and interglycosidic linkage of disaccharides on the properties of proline-rich antimicrobial glycopeptides, formaecin I and drosocin. Their glycosylated analogs-bearing lactose, maltose and cellobiose, as a glycan side chain on their conserved threonine residue, were synthesized where these disaccharides possess identical proximal sugar and vary in the nature of distal sugar and/or interglycosidic linkage. The structural and functional properties of these disaccharide-containing formaecin I and drosocin analogs were compared with their corresponding monoglycosylated forms, β-D-glucosyl-formaecin I and β-D-glucosyl-drosocin, respectively. We observed neither major secondary structural alterations studied by circular dichroism nor substantial differences in the toxicity with mammalian cells among all of these analogs. The comparative analyses of antibacterial activities of these analogs of formaecin I and drosocin displayed that β-D-maltosyl-formaecin I and β-D-maltosyl-drosocin were more potent than that of respective β-D-Glc-analog, β-D-cellobiosyl-analog and β-D-lactosyl-analog. Despite the differences in their antibacterial activity, all the analogs exhibited comparable binding affinity to DnaK that has been reported as one of the targets for proline-rich class of antibacterial peptides. The comparative–quantitative internalization studies of differentially active analogs revealed the differences in their uptake into bacterial cells. Our results exhibit that the sugar chain length as well as interglycosidic linkage of disaccharide may influence the antibacterial activity of glycosylated analogs of proline-rich antimicrobial peptides and the magnitude of variation in antibacterial activity depends on the peptide sequence.

Additional supporting information may be found in the online version of this article at the publisher's web site.

Keywords: glycosylation; disaccharide; antibacterial peptide; proline-rich

Introduction

Glycosylation is an important post-translational modification affecting protein stability, structure, interactions and function [1,2]. These effects depend on a variety of factors associated with glycosylation. The size of glycan attached to the protein is also one of the factors that influence the physicochemical and biological properties of protein. It has been earlier observed that increasing the degree of glycosylation and glycan size helps in protein stability [3]. The length of sugar chain can have complex impact on peptide/protein structure as well as function [4]. The structural or/and functional effects of sugar chain have been studied with small synthetic glycopeptides. The structural studies of a mucin fragment from CD43 by NMR [4] suggested that the distal sugar residues did not influence the overall peptide conformation; whereas in another report, detailed comparative structural analysis of two distinct peptides reported the differential effect of a mono – or a disaccharide on their backbone conformations confirming the importance of sugar chain length [5]. The functional consequences of glycan chain length in a glycopeptide were studied for T-helper cell epitope, and its stimulatory ability was found to be hampered with extended sugar chain [6]. In case of CLV3 glycopeptide, its biological activity increased progressively as the sugar chain length increased [7]. Thus, carbohydrate length may play a key role in modulating the biological activity of glycopeptide probably by affecting the structure and stabilizing the different conformations. It has been reported that the impact of sugar chain is highly specific for the sequence of amino acids [8,9].

The proline-rich antimicrobial peptides (AMPs) include *O*-glycosylated AMPs like drosocin [10], pyrrhocoricin [11], formaecins [12] and so on that carry carbohydrate moiety at their conserved threonine residue. Unlike other antibacterial peptides that kill bacteria by lysing their cell membrane, this group of AMPs are known to be transported stereospecifically into the cytoplasm and inhibiting specific intracellular targets [13]. DnaK, a bacterial heat-shock protein, has been suggested to be one of the target molecules for this class of AMPs [14]. It has been reported earlier that *O*-glycosylation

* *Correspondence to: Kanwal J. Kaur, Structural Biology Unit, National Institute of Immunology, Aruna Asaf Ali Marg, New Delhi 110 067, India. E-mail: kanwal@nii.ac.in*

† *Deepti S. Lele and Rohini Dwivedi contributed equally to this work.*

Structural Biology Unit, National Institute of Immunology, Aruna Asaf Ali Marg, New Delhi 110 067, India

has an effect on the conformation and biological activity of these antibacterial peptides [15–18]. Importance of α-D-GalNAc for the activity of drosocin has been previously reported by Gobbo *et al.* [17]. They have shown that in monoglycosylated drosocin, the substitution of α-D-GalNAc attached to threonine by α-D-Gal or β-D-Gal resulted in the reduction of its antibacterial activity. Earlier, we have also reported the consequences of variation of sugar and its linkage to threonine residue in the antibacterial activities of formaecin I and monoglycosylated drosocin (M-drosocin) [18]. Differences in the antibacterial activity of the differentially glycosylated analogs of formaecin I and drosocin have been suggested because of variation in conformation of peptides due to topological differences among sugar moieties affecting their binding to the bacterial targets. In the present report, we have synthesized analogs of formaecin I and drosocin carrying maltose, cellobiose and lactose as side chain attached to threonine. Interestingly, all of these disaccharides share common proximal sugar, i.e. β-D-glucose, but they differ in the nature of distal sugar and/or interglycosidic linkage. We have examined the effect of distal sugar/sugar chain length of formaecin I and M-drosocin on their antibacterial activities as well as cytotoxic properties to mammalian cells. We have also studied the binding kinetics of these peptides with heat-shock protein, DnaK using surface plasmon resonance and bacterial uptake of their fluorescently labeled analogs. Secondary structural analysis of the peptides was performed using circular dichroism (CD). Thus, these antibacterial glycopeptides provide useful model system for studying the effect of differential disaccharides on their structural and functional properties.

Materials and Methods

Peptide Synthesis

All the peptides used in this study were chemically synthesized by fluorenylmethyloxycarbonyl (Fmoc) solid-phase synthesis [19] on an automated peptide synthesizer (433A; Applied Biosystems, Foster City, CA, USA). For synthesis of glycosylated peptides, presynthesized glycosylated amino acid was added and coupled manually on growing polypeptide chain. Fluorescein-labeled peptides were synthesized after the addition of lysine at the *N*-terminus of peptide, and then fluorescein group was attached at the free *N*-terminal α-amino group. The peptides were cleaved from the peptide-resin by treatment with a cleavage mixture of phenol (0.75 g): 1,2-ethanedithiol (0.25 ml): TFA (10 ml): thioanisole (0.5 ml): water (0.5 ml). The crude peptides were purified by reverse phase semi-preparative HPLC (Waters, USA) using C18 column (Waters XBRIDGE™ BEH 130 reverse phase C18 column, 19 × 250 mm, 10 μm, spherical) as reported previously [20]. The purified glycosylated peptides were deacetylated using aqueous 5% hydrazine hydrate and then purified again using HPLC. The synthesized peptides were determined to be >95% pure by HPLC (Supporting Information). The peptides were characterized using mass spectrometry.

General Procedure for Glycosylation of Fmoc-Threonine Benzyl Ester

A mixture of Fmoc-Thr-OBzl (1 mmol), per-*O*-acetylated trichloroacetimidate of sugar (**1**) or (**2**) or (**3**) (1.3 mmol) and activated 4 A° molecular sieves in dry CH_2Cl_2, was stirred at room temperature for 30 min under argon. Trimethylsilyl trifluoromethanesulfonate (0.01 mmol) was added at 0 °C, and the reaction mixture was stirred at room temperature until completion indicated by TLC (1 : 1 hexane: ethyl acetate). The mixture was diluted with CH_2Cl_2 and quenched with triethylamine. The reaction mixture was filtered, washed with saturated $NaHCO_3$ and H_2O and dried over $MgSO_4$. The crude product was purified by flash chromatography. The appropriate fractions were combined and concentrated to give the desired product. All the products were characterized by ESI-high-resolution mass spectrometry (HRMS), ^1H and ^{13}C NMR spectroscopy (Supporting Information).

*N^{α}-Fluoren-9-ylmethoxycarbonyl-O-(2,3,4,6-tetra-O-acetyl-α-D-glucopyranosyl-(1->4)-2,3,6-tri-O-acetyl-β-D-glucopyranosyl)-L-threonine benzyl ester (**4**)*

Purification by flash chromatography (gradient of 0–50% EtOAc-hexane over 40 min) afforded **4** (6.2 g, 71%) as a white solid. ^1H NMR (300 MHz, $CDCl_3$) δ7.76 (d, J = 7.4 Hz, 2H, Ar), 7.63 (d, J = 7.4 Hz, 2H, Ar), 7.42–7.28 (m, 9H, Ar), 5.65 (d, J = 9.4 Hz, 1H, NH), 5.42–5.24 (m, 4H, h-3′, h-1′, OCH_2Ph), 5.19–5.04 (m, 3H, h-4′, H-3), 4.86 (dd, J = 4.0, 10.6 Hz, 1H, H-2), 4.74 (t, J = 8.2, 9.2 Hz, 1H, CH-Thrα), 4.48–4.32 (m, 5H, $FmocCH_2$, FmocCH, H-1, H-6a), 4.29–4.22 (m, 2H, H-6b, CHFmocβ), 4.13–3.89 (m, 4H, H-6′a, H-6′b, H-4, H-5′), 3.23–3.20 (m, 1H, H-5), 2.09, 2.08, 2.06, 2.04, 2.01, 2.00 (6s, 21H, 7Ac), 1.22 (d, J = 6.0 Hz, 3H, Thr-CH_3). ^{13}C NMR (75 MHz, $CDCl_3$): δ 170.65, 170.64, 170.54, 170.34, 170.12, 169.90, 169.63 (COCH3), 169.54, 157.23 (CO Fmoc), 144.03, 143.90, 141.43, 135.58, 128.93, 128.84, 128.57, 127.86, 127.24, 125.37, 120.10 (Ar C), 98.57 (C-1), 95.66 (C-1′), 75.61, 75.47, 72.39, 72.17, 70.22, 69.32, 68.68, 68.13, 67.52, 62.62, 61.57, 58.74, 53.80, 47.32, 21.05, 20.85, 20.80, 20.73, 17.71 (CH_3 Thr). ESI HRMS: calcd for $C_{52}H_{59}NO_{22}[M+H]^+$ m/z, 1050.3607; found, 1050.2822.

*N^{α}-Fluoren-9-ylmethoxycarbonyl-O-(2,3,4,6-tetra-O-acetyl-α-D-glucopyranosyl-(1->4)-2,3,6-tri-O-acetyl-β-D-glucopyranosyl)-L-threonine (**I**)*

To a solution of **4** (3.75 g) in ethyl acetate, 150 ml was added 10% Pd/C (1 g). The mixture was stirred under one atmosphere of hydrogen gas until the reaction was complete. The catalyst was removed by filtration, and after solvent evaporation, the residue was purified by flash chromatography using DCM as solvent A and 10% MeOH-DCM as solvent B (gradient of 0–40% B over 35 min) to afford **I** (2 g, 60%). ^1H NMR (300 MHz, $CDCl_3$): δ 7.77 (d, J = 7.4 Hz, 2H, Ar), 7.65–7.60 (m, 2H, Ar), 7.43–7.29 (m, 4H, Ar), 5.55 (d, J = 9.6 Hz, 1H, NH), 5.46 (d, J = 3.9 Hz, 1H, H-1′), 5.38 (t, J = 9.9 Hz, 1H, H-3′), 5.30 (t, J = 12.1 Hz, 1H, H-3), 5.23 (t, J = 9.1 Hz, 1H, H-4′), 5.07 (t, J = 9.8 Hz, 1H, H-2′), 4.92–4.75 (m, 3H, $FmocCH_2$, H-2), 4.55 (d, J = 7.8 Hz, 1H, H-1), 4.45–4.37 (m, 3H, FmocCH, CHFmocα, CHFmocβ), 4.33–4.23 (m, 2H, H-6a, H-6b), 4.18–3.97 (m, 4H, H-6′a, H-6′b, H-4, H-5′), 3.60–3.57 (m, 1H, H-5), 2.21, 2.11, 2.05, 2.03, 2.01 (5s, 21H, 7Ac), 1.21 (d, J = 6.2 Hz, 3H, Thr-CH_3); ^{13}C NMR (75 MHz, $CDCl_3$) δ 172.55, 171.30, 170.83, 170.71, 170.46, 170.22, 169.68 ($COCH_3$), 169.60, 156.93 (CO Fmoc), 144.06, 143.91, 141.45, 127.90, 127.30, 125.41, 120.15 (Ar C), 99.57 (C-1), 95.53 (C-1′), 76.66, 75.14, 72.50, 72.10, 70.31, 69.44, 68.57, 68.21, 67.57, 61.88, 61.62, 58.20, 53.63, 47.29, 47.1, 21.34, 21.09, 20.89, 20.80, 20.77, 20.74 ($COCH_3$), 17.82 (CH_3 Thr). ESI HRMS: calcd for $C_{45}H_{53}NO_{22}$ $[M+H]^+$ m/z, 960.3137; found, 960.3132.

*N^{α}-Fluoren-9-ylmethoxycarbonyl-O-(2,3,4,6-tetra-O-acetyl-β-D-glucopyranosyl-(1->4)-2,3,6-tri-O-acetyl-β-D-glucopyranosyl)-threonine benzyl ester (**5**)*

The crude residue was purified by flash chromatography using gradient of 0–60% EtOAc-hexane over 40 min, to give the titled

Journal of PeptideScience

compound **5** (4.8 g, 69%). ^{1}H NMR (300 MHz, $CDCl_3$) δ7.77 (d, J = 7.4 Hz, 2H, Ar), 7.63 (d, J = 7.3 Hz, 2H, Ar), 7.42–7.27 (m, 9H, Ar), 5.67 (d, J = 9.3 Hz, 1H, NH), 5.30 (s, 2H, OCH_2Ph), 5.19–5.04 (m, 3H, H-2′, H-3, H-3′, H-4′), 4.96–4.81 (m, 2H, H-2, CHThrα), 4.53–4.33 (m, 7H, H-1′, H-1, FmocCH$_2$, CHThrβ, H-6a, H-6′a), 4.24 (t, 1H, J = 7.2 Hz, FmocCH), 4.07–3.97 (m, 2H, H-6b, H-6′b) 3.74–3.64 (m, 2H, H-4, H-5′), 3.34–3.30 (m, 1H, H-5), 2.10, 2.05, 2.04, 2.03, 2.01, 1.99 (6s, 21H, 7Ac), 1.21 (d, J = 6.2 Hz, 3H, Thr-CH_3). ^{13}C NMR (75 MHz, $CDCl_3$): δ 170.65, 170.44, 170.38, 169.99, 169.95, 169.63, 169.48 (COCH3), 169.23, 156.91 (CO Fmoc), 144.13, 143.88, 141.44, 135.53, 128.83, 128.77, 128.35, 127.87, 127.24, 125.39, 120.12 (Ar C), 100.94 (C-1), 98.78 (C-1′) 76.36, 75.29, 73.09, 72.73, 72.32, 72.14, 71.74, 71.61, 67.96, 67.48, 67.40, 61.76, 58.59, 47.30, 20.89, 20.83, 20.74, 20.71 (COCH3), 17.46 (CH_3 Thr). ESI HRMS: calcd for $C_{52}H_{59}NO_{22}[M+H]^+$ m/z, 1050.3607; found, 1050.2557.

*N$^{\alpha}$-Fluoren-9-ylmethoxycarbonyl-O-(2,3,4,6-tetra-O-acetyl-β-D-glucopyranosyl-(1->4)-2,3,6-tri-O-acetyl-β-D-glucopyranosyl)-L-threonine (**II**)*

A mixture of **5** (1.6 g) and 10%Pd/C (700 mg) in ethyl acetate was treated as described for the synthesis of **I**. Purification by flash chromatography using DCM as solvent A and 10% MeOH-DCM as solvent B (gradient of 0–50% B over 40 min) to afford **II** (990 mg, 68%) as a white solid. ^{1}H NMR (300 MHz, CD_3OD): δ 7.81 (d, J = 7.4 Hz, 2H, Ar), 7.70–7.67 (m, 2H, Ar), 7.42–7.29 (m, 4H, Ar), 5.25 (t, J = 9.4 Hz, 1H, H-3), 5.18 (t, J = 9.3 Hz, 1H, H-3), 5.01 (t, J = 9.6 Hz, 1H, H-4′), 4.85–4.78 (m, 2H, H-2′, H-2), 4.68 (d, J = 7.9 Hz, 1H, H-1′), 4.67 (d, J = 7.9 Hz, 1H, H-1), 4.51–4.32 (m, 5H, CHFmocα, FmocCH$_2$, H-6a, H-6′a), 4.27–4.20 (m, 2H, H-6′b, FmocCH), 4.15–4.02 (m, 2H, H-4, H-6b), 3.89–3.81 (m, 2H, H-5′, CHThrβ), 3.73–3.68 (m, 1H, H-5), 2.09, 2.05, 2.04, 2.03, 2.01, 1.99, 1.94 (7s, each 3H, 7Ac), 1.19 (d, J = 6.3 Hz, 3H, Thr-CH_3); ^{13}C NMR (75 MHz, CD_3OD) δ 173.37, 172.70, 172.32, 172.00, 171.76, 171.57, 171.32, 171.08, 158.93 ($COCH_3$ and CO Fmoc), 145.46, 145.27, 142.75, 128.99, 128.37, 126.47, 121.13 (Ar C), 102.06 (C-1), 100.17 (C-1′), 78.07, 76.58, 74.59, 74.23, 73.99, 73.24, 73.07, 69.43, 68.31, 63.64, 62.96, 59.90, 54.95, 21.10, 20.95, 20.90, 20.83, 20.79, 20.69 ($COCH_3$), 17.94 (CH_3 Thr). ESI HRMS: calcd for $C_{45}H_{53}NO_{22}$ $[M+H]^+$ m/z, 960.3137; found, 960.2976.

*N$^{\alpha}$-Fluoren-9-ylmethoxycarbonyl-O-(2,3,4,6-tetra-O-acetyl-β-D-galactopyranosyl-(1->4)-2,3,6-tri-O-acetyl-β-D-glucopyranosyl)-L-threonine benzyl ester (**6**)*

Purification of crude residue by flash chromatography (gradient of 0–60% EtOAc-hexane over 60 min) afforded **6** (2.25 g, 70%) as an amorphous white solid. ^{1}H NMR (300 MHz, $CDCl_3$): δ 7.76 (d, J = 7.5 Hz, 2H, Ar), 7.63 (d, J = 7.5 Hz, 2H, Ar), 7.42–7.28 (m, 9H, Ar), 5.64 (d, J = 9.3 Hz, 1H, NH), 5.36 (1H, d, J = 3.1 Hz, H-4′), 5.30 (2H, br s, OCH_2Ph), 5.20–5.08 (m, 3H, H-2′, H-2, H-3), 4.95 (dd, J = 10.4, 3.4 Hz, 1H, H-3′), 4.86–4.81 (m, 1H, CHThrα), 4.46–4.33 (m, 6H, H-1′, H-1, FmocCH$_2$, H-6b, H-6′b), 4.24 (t, J = 7.3 Hz, 1H, Fmoc CH), 4.17–4.05 (m, 2H, H-6′a, CHThrβ), 4.01 (dd, J = 12.1, 4.8 Hz, 1H, H-6a), 3.87–3.82 (m, 1H, H-5′), 3.73 (t, J = 9.4 Hz, 1H, H-4), 3.38–3.34 (m, 1H, H-5), 2.16, 2.07, 2.06, 2.05, 2.04, 1.97 (6s, 21H, 7Ac), 1.21 (d, J = 6.1 Hz, 3H, Thr-CH_3); ^{13}C NMR (75 MHz, $CDCl_3$): δ 170.57, 170.34, 170.27, 170.03, 169.97, 169.69, 169.28 ($COCH_3$), 156.95 (CO Fmoc), 144.19, 143.94, 141.5, 135.58, 128.88, 128.80, 128.39, 127.92, 127.29, 125.44, 120.17 (Ar C), 101.28 (C-1), 98.78 (C-1′), 77.43, 76.19, 75.31, 72.78, 72.69, 71.77, 71.20, 70.94, 69.29, 67.55, 67.45, 66.85, 61.95, 61.07, 58.68, 53.63, 47.37, 21.02, 20.94, 20.86, 20.72 ($COCH_3$), 17.48 (CH_3 Thr). ESI HRMS: calcd for $C_{52}H_{59}NO_{22}[M+H]^+$ m/z, 1050.3607; found, 1050.3026.

*N$^{\alpha}$-Fluoren-9-ylmethoxycarbonyl-O-(2,3,4,6-tetra-O-acetyl-β-D-galactopyranosyl-(1->4)-2,3,6-tri-O-acetyl-β-D-glucopyranosyl)-L-threonine (**III**)*

To a solution of **6** (2 g) in methanol, 100 ml was added 5% Pd/C (400 mg). The mixture was stirred under one atmosphere of hydrogen gas until the reaction was complete. The catalyst was removed by filtration, and after solvent evaporation, the residue was purified by flash chromatography using DCM as solvent A and 10% MeOH-DCM as solvent B (gradient of 0–60% B over 50 min) to afford the titled compound **III** (1.2 g, 65%). ^{1}H NMR (300 MHz, CD_3OD): δ 7.79 (d, J = 7.5 Hz, 2H, Ar), 7.69–7.65 (m, 2H, Ar), 7.42–7.29 (m, 4H, Ar), 5.36 (d, J = 3.1 Hz, 1H, H-4′), 5.19 (t, J = 9.2 Hz, 1H, H-3), 5.21 (dd, J = 10.3, 3.2 Hz, 1H, H-3′), 5.03 (dd, J = 10.3, 7.7 Hz, 1H, H-2′), 4.86–4.78 (m, 3H, FmocCH$_2$, H-2), 4.66 (d, J = 7.4 Hz, 1H, H-1′), 4.65 (d, J = 7.6 Hz, 1H, H-1), 4.49–4.32 (m, 3H, Fmoc CH, CHThrβ, CHThrα), 4.28–4.21 (m, 2H, H-6a, H-6′a), 4.17–4.09 (m, 3H, H-5′, H-6b, H-6′b), 3.84 (t, J = 9.1 Hz, 1H, H-4), 3.72–3.65 (m, 1H, H-5), 2.12, 2.08, 2.06, 2.03, 2.01, 1.94 (6s, 21H, 7Ac), 1.18 (d, J = 6.0 Hz, 3H, Thr-CH_3); ^{13}C NMR (75 MHz, CD_3OD) δ 173.27, 172.63, 172.14, 172.04, 171.79, 171.56, 171.22 ($COCH_3$), 158.77 (CO Fmoc), 145.40, 145.19, 142.64, 128.97, 128.35, 126.44, 121.13 (Ar C), 102.12 (C-1), 100.06 (C-1′), 77.63, 76.55, 74.35, 73.85, 73.13, 72.51, 71.86, 70.79, 68.69, 68.21, 63.64, 62.51, 61.64, 59.81, 54.97, 48.49 (CH Fmoc), 21.30, 20.99, 20.96, 20.92, 20.82, 20.68 ($COCH_3$), 17.96 (CH_3 Thr). ESI HRMS: calcd for $C_{45}H_{53}NO_{22}$ $[M+H]^+$ m/z, 960.3137; found, 960.3051.

Broth Microdilution Assay

Minimum inhibitory concentrations (MICs) of peptides against various bacterial strains such as *Escherichia coli* ATCC 35218, *E. coli* ATCC 25922, *E. coli* ATCC 11775, *Salmonella typhimurium* ATCC 14028 and *S. typhi* Vi+ were determined following the earlier reported protocol [20]. Each test condition was set up in duplicate, and the assay was repeated thrice to calculate the average and the standard error.

Binding Kinetics by Surface Plasmon Resonance

Binding studies between substrate binding domain-DnaK (substrate binding domain of DnaK-*E. coli*) and glycosylated analogs of formaecin I and drosocin were performed on Biacore™ T-200 (Biacore, Uppsala, Sweden) following the earlier described protocol of covalent immobilization of His^6-tagged protein on nickel-nitrilotriacetic acid sensor chip [21,22]. The reference surface was treated in the same way, but no ligand was immobilized on this surface. For binding kinetics, an injection of each peptide with concentration ranging from 5 μM–156 nM was passed over immobilized surfaces, allowing an association time of 180 s and disassociation time of 900 s followed by two regeneration injections of 15 s each with 500 mM NaCl. All the experiments were performed at 25 °C. The reference-subtracted response curves obtained for peptide binding were evaluated using Biacore T-200 evaluation software (Biacore). The data obtained with serially diluted peptide concentrations were fitted in Langmuir 1 : 1 interaction model to obtain rates of association (k_{ass}) and dissociation (k_{diss}). The equilibrium dissociation constant (K_D) was defined

as the ratio of the dissociation rate constant (k_{diss}) and the association rate constant (k_{ass}).

Internalization of Labeled Peptides into Bacteria Using Fluorescence-Activated Cell Sorting (FACS) Analysis

Fluorescein isothiocyanate (FITC)-labeled formaecin I and drosocin-bearing β-D-glucosyl and β-D-maltosyl were synthesized and studied for their internalization in *E. coli* ATCC25922 cells by flow cytometry (FACS, Becton Dickinson) following the earlier reported protocol [22]. The influx of propidium iodide (PI), a DNA-staining fluorescent probe and FITC-labeled peptides into bacterial cells were investigated by using dual-laser fluorescence-activated cell sorter. For sample preparation, the mid-logarithmic phase *E. coli* cells were washed twice with phosphate buffer (PB) (10 mM, pH 7.4). Cell density was adjusted to 10^8 cells/ml in lysogeny broth media. A total of 200 µl of these cells was incubated with FITC-labeled formaecin (10 µM) and drosocin (4 µM) peptide analogs at 26 °C for different time intervals (10, 30 and 60 min). Cells were washed thrice with ice-cold phosphate-buffered saline (PBS) and resuspended in 200 µl of PBS. The PI staining of the cells was performed using 1 µl of PI (1 mg/ml) to determine the cell viability. The samples were analyzed by flow cytometry using the software FLOWJO (FlowJo, Ashland, OR, USA). Untreated bacterial cells were used to set up the gating parameters.

CD Spectroscopy

The CD spectra of all peptides (50 µM) were obtained at 25 °C in a 1-mm pathlength cuvette in the range of 250–190 nm using CD spectrometer (J-815, JASCO Corporation, Tokyo, Japan). Five scans with a speed of 100 nm/min were averaged and analyzed using JASCO spectra analysis software. The spectra were recorded in 10 mM PB pH 7.4, 90% TFE in water, 10 mM SDS and 50 µM lipopolysaccharide (LPS) (*S. typhimurium,* Sigma) in 10 mM PB pH 7.4. The buffer, 90% TFE, 10 mM SDS or 50 µM LPS background was subtracted from the experimental data. Results were expressed as mean residue ellipticity in [θ] (Deg-cm^2/dmol).

Hemolytic Assay

Hemolytic assay was performed following the earlier reported protocol [18]. In brief, a 200-µl aliquot of packed rat erythrocytes volume was washed with cold PBS (10 mM PB, pH 7.4, 150 mM NaCl) at 4 °C until the supernatant was colorless that was discarded each time. The pellet was resuspended in PBS, diluting the cells to 2% of their packed volume. The erythrocytes (90 µl) were plated in a 96-well microtiter plate (Greiner Bio-One, Wemmel, Belgium) along with 10 µl of peptide solution corresponding to final concentration of 200 µM added to the wells, and the plate was incubated at 37 °C for 90 min. Any hemolytic activity would manifest as rupture of red blood cells (RBCs) and release of hemoglobin into the solution. Subsequently, the plate was centrifuged at 4000 rpm for 10 min to pellet intact cells, and 75 µl of supernatant was transferred to a flat bottom microtiter plate (Greiner Bio-One, Wemmel, Belgium). Its absorbance was read at 405 nm, and the percentage of RBCs' lysis was calculated. The hemolysis affected by only PBS and 1% TritonX-100 was considered as negative control and 100% hemolysis, respectively. Each test condition was set up in triplicate, and the results have been averaged from three independent experiments.

MTT Assay

Cytotoxicity of the synthetic peptides was determined by standard methylthiazolyldiphenyl tetrazolium bromide (MTT) assay following the earlier reported protocol [18]. The method is based on the reduction of the salt, MTT into a crystalline blue formazan product by the cellular oxidoreductases of viable cells. The synthesized peptides were incubated with murine macrophages cell line, J774 (2.5×10^4 cells/well). Following 24 h incubation with peptides (1 mg/ml), cells were washed and then incubated with fresh culture media and 100 µl MTT (Sigma, 5 mg/ml) in 0.1 M PBS, pH 7.4 at 37 °C in a humid atmosphere with 5% CO_2 for 4 h. Media was then gently aspirated from test cultures, and 100 µl of dimethyl sulfoxide was added to all wells. The plates were then shaken for 2 min, and the absorbance was read at 570/630 nm in a microtiter plate reader. The percentage of viability was calculated as AT/AC × 100, where AT and AC are the absorbances of treated and negative control cells, respectively. In the positive and negative controls, the peptide solution was substituted by the same volumes of ethanol and PBS, respectively. Each test condition was set up in triplicate, and the results have been averaged from three independent experiments.

Results and Discussion

Synthesis and Characterization of Antibacterial Glycopeptides Containing Disaccharides

To investigate the effect of glycan chain length on the structure and function of antibacterial glycopeptides, formaecin I and M-drosocin, we have synthesized their analogs consisting of maltose, cellobiose and lactose as glycan side chains attached to threonine. All these disaccharide containing antibacterial glycopeptides have as proximal sugar β-D-glucose that is *O*-linked to threonine, but they differ in the nature of distal sugar and/or interglycosidic linkage. The synthesis of these analogs of formaecin I and drosocin was achieved in two steps: (i) synthesis of glycosylated building blocks and (ii) incorporation of the glycosylated amino acid into the peptide.

For synthesizing glycosylated building blocks (Figure 1), N^{α}-Fmoc-Thr(Ac$_7$-β-D-maltose)-OH (**I**), N^{α}-Fmoc-Thr(Ac$_7$-β-D-cellobiose)-OH (**II**) and N^{α}-Fmoc-Thr(Ac$_7$-β-D-lactose)-OH (**III**), first, the per-*O*-acetylated saccharides were converted into their corresponding 1-*O*-unprotected pyranoses that were transformed with trichloroacetonitrile in the presence of base following the earlier reported protocol [23], into their corresponding trichloroacetimidates. The glycosylation of N^{α}-Fmoc-benzyl-protected threonine with per-*O*-acetylated trichloroacetimidates of maltose (**1**), cellobiose (**2**) and lactose (**3**) in the presence of catalytic amounts of trimethylsilyl trifluoromethanesulfonate afforded high yield of β-linked glycosides **4, 5** and **6**, respectively. Finally, benzyl esters of **4, 5** and **6** were reduced with Pd/C under H_2 atmosphere, which provided the desired products **I, II** and **III**, respectively (Scheme 1).

The resulting glycosylated threonine building blocks were used for synthesizing glycosylated analogs of formaecin I and drosocin. The glycopeptides were synthesized by following the solid phase methodology. Briefly, the peptide chain was first assembled on the resin by standard Fmoc/DCC-HOBt protocol until the glycosylated threonine residue position. The glycosylated threonine was then coupled to the NH_2-peptide resin by Fmoc/HBTU protocol [24]. Further elongation of the peptide chain was carried out according to the standard Fmoc/DCC-HOBt protocol. For fluorescein-labeled peptides, fluorescein was added

Journal of PeptideScience

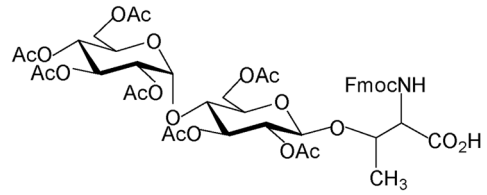

N^{α}-Fmoc-Thr(Ac_7-β-D-Maltose)-OH (I)

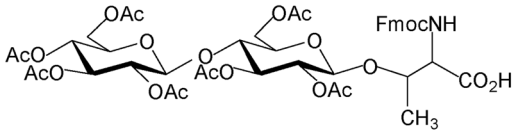

N^{α}-Fmoc-Thr(Ac_7-β-D-Cellobiose)-OH (II)

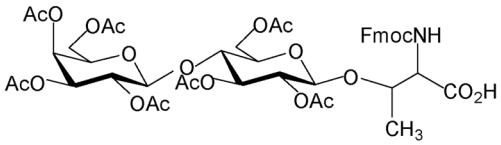

N^{α}-Fmoc-Thr(Ac_7-β-D-Lactose)-OH (III)

Figure 1. Illustrations of glycosylated amino acids that were chemically synthesized.

after the extra lysine residue coupled at the *N*-terminus. The deprotection and cleavage of peptides from resin provided the glycopeptides with acetyl groups-protected sugar. The purified glycosylated peptides were deacetylated by their treatment with 5% hydrazine hydrate. Finally, all the peptides were repurified and characterized by mass spectrometry (Table 1; also, see Supporting Information).

Earlier, we have reported the antibacterial potential, hemolytic and cytotoxic activities of β-D-glucosyl-formaecin I and β-D-glucosyl-drosocin as well as their structural features by CD studies [18]. In this report, we have compared the structural and functional properties of disaccharide containing analogs of formaecin I and drosocin with that of their corresponding monoglycosylated counterparts, i.e. β-D-glucosyl-formaecin I and β-D-glucosyl-drosocin, respectively, to investigate the effect of distal sugar and interglycosidic linkage.

Antibacterial Activity

The antimicrobial activities of β-D-maltosyl-analog, β-D-cellobiosyl-analog and β-D-lactosyl-analog of formaecin I and drosocin were compared with their corresponding monoglycosylated forms, β-D-glucosyl-formaecin I and β-D-glucosyl-drosocin, respectively, by analyzing their MIC against Gram-negative bacterial strains like *E. coli* ATCC 35218, *E. coli* ATCC 25922, *E. coli* ATCC 11775, *S. typhimurium* ATCC 14028 and *S. typhi* Vi+. All disaccharide analogs of formaecin I and drosocin and their monoglycosylated counterparts exhibited strain-specific antibacterial activities. β-D-maltosyl-formaecin I and β-D-maltosyl-drosocin displayed higher antibacterial activity in comparison with that of their respective other disaccharide and monosaccharide containing analogs (Figures 2A and 2B). β-D-maltosyl-formaecin I having α-nature of interglycosidic linkage in its disaccharide showed around two times lower MIC in comparison with that of β-D-glucosyl-formaecin I against all the tested bacterial strains of *E. coli* and *Salmonella*. β-D-cellobiosyl-formaecin I and β-D-lactosyl-formaecin I containing different terminal sugars in their disaccharides linked to threonine but similar interglycosidic linkage (β) showed the similar antibacterial activity against all the tested bacterial strains. Moreover, these two analogs of formaecin I resulted in MIC values comparable with that of β-D-glucosyl-formaecin I against the Gram-negative bacterial strains of *E. coli* and *S. typhi* Vi+ but exhibited marginally higher MIC values against *S. typhimurium* ATCC14028 in comparison with that of β-D-glucosyl-formaecin I. β-D-maltosyl-formaecin I that differed in the nature of interglycosidic linkage from the other two disaccharide containing formaecin analogs displayed around two times higher antibacterial activity in comparison with that of β-D-cellobiosyl-formaecin I and β-D-lactosyl-formaecin I against all the tested bacterial strains (Figure 2A).

The effect of sugar chain length on the antibacterial activity of drosocin analogs was also analyzed and compared with that of β-D-glucosyl-drosocin using the aforementioned Gram-negative bacterial strains (Figure 2B). β-D-maltosyl-drosocin exhibited MIC value lower than that of β-D-glucosyl-drosocin against bacterial strains of *E. coli* and *Salmonella*. β-D-cellobiosyl-drosocin displayed antibacterial activity almost comparable with β-D-glucosyl-drosocin against *E. coli* strains but showed higher antibacterial activity than that of β-D-glucosyl-drosocin against *Salmonella* strains. β-D-lactosyl-drosocin that differed in the nature of distal sugar from β-D-cellobiosyl-drosocin displayed antibacterial activity slightly higher than that of this analog as well as respective monoglycosylated analog, β-D-glucosyl-drosocin against all the tested bacterial strains (Figure 2B).

The aforementioned results indicated that the antimicrobial potentials of β-D-maltosyl-formaecin I and β-D-maltosyl-drosocin were higher than that of their respective monoglycosylated analogs. The magnitude of variation in antibacterial activity was more

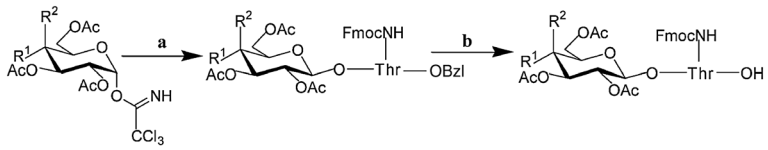

1 R^1 = H, R^2 = Glc(OAc_4)-α-O
2 R^1 = Glc(OAc_4)-β-O, R^2 = H
3 R^1 = Gal(OAc_4)-β-O, R^2 = H
4 R^1 = H, R^2 = Glc(OAc_4)-α-O
5 R^1 = Glc(OAc_4)-β-O, R^2 = H
6 R^1 = Gal(OAc_4)-β-O, R^2 = H
I R^1 = H, R^2 = Glc(OAc_4)-α-O
II R^1 = Glc(OAc_4)-β-O, R^2 = H
III R^1 = Gal(OAc_4)-β-O, R^2 = H

[a]Reagents and conditions: (a) CH_2Cl_2, Fmoc-Thr-OBn,TMSOTf; (b) H_2, 10%Pd/C, EtOAc/MeOH

Scheme 1. Synthesis of glycosylated threonine building blocks.

Table 1. Amino acid sequences and mass characterization of glycosylated analogs of formaecin I and drosocin

Peptide name	Sequence	MALDI-TOF MS [M+H]calcd	MALDI-TOF MS [M+H]exptl
β-D-glucosyl-formaecin I	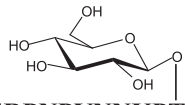 GRPNPVNNKPTPHPRL	1956.0425	1956.0729
β-D-maltosyl-formaecin I	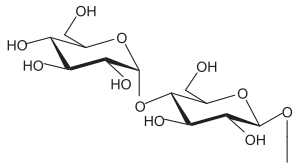 GRPNPVNNKPTPHPRL	2118.0953	2118.1213
β-D-cellobiosyl-formaecin I	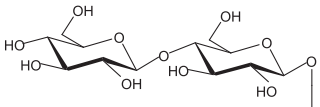 GRPNPVNNKPTPHPRL	2118.0953	2118.1108
β-D-lactosyl-formaecin I	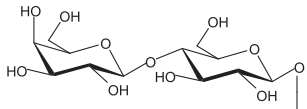 GRPNPVNNKPTPHPRL	2118.0953	2118.1062
β-D-glucosyl-drosocin	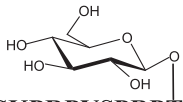 GKPRPYSPRPTSHPRPIRV	2360.3766	2360.3701
β-D-maltosyl-drosocin	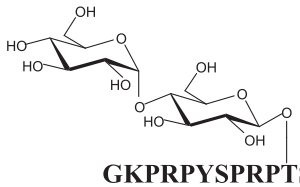 GKPRPYSPRPTSHPRPIRV	2522.3492	2522.3896
β-D-cellobiosyl-drosocin	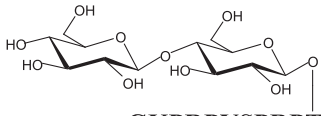 GKPRPYSPRPTSHPRPIRV	2522.3492	2522.3279
β-D-lactosyl-drosocin	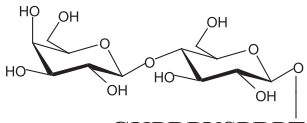 GKPRPYSPRPTSHPRPIRV	2522.3492	2522.3547
FITC-β-D-glucosyl-formaecin I	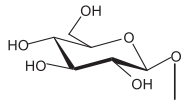 FITC-KGRPNPVNNKPTPHPRL	2441.1774[a]	2441.1392
FITC-β-D-maltosyl-formaecin I	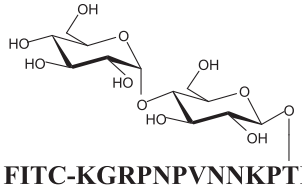 FITC-KGRPNPVNNKPTPHPRL	2603.2302[a]	2603.1968
FITC-β-D-glucosyl-drosocin		2845.5115[a]	2845.3456

Journal of PeptideScience

Table 1. *(Continued)*

Peptide name	Sequence	MALDI-TOF MS [M+H]calcd	MALDI-TOF MS [M+H]exptl
FITC-β-D-maltosyl-drosocin	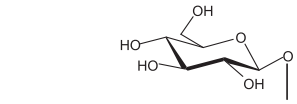 FITC-KGKPRPYSPRPTSHPRPIRV	3007.4841[a]	3007.2190

[a]ESI-HRMS [M+]

pronounced in formaecin analogs than in glycosylated analogs of drosocin, confirming that the effect of glycosylation depends on the peptide sequence as reported earlier [8,18]. Moreover, β-D-maltosyl-formaecin I and β-D-maltosyl-drosocin were more potent than β-D-cellobiosyl-formaecin and β-D-cellobiosyl-drosocin, respectively, in spite of having the same peptide and sugar sequence but differ only in respect to interglycosidic linkage of their disaccharide. Even β-D-maltosyl-bearing analogs of formaecin I and drosocin displayed higher antibacterial activity than that of corresponding β-D-lactosyl-analogs that differ in the nature of distal sugar along with the interglycosidic linkage from one another. These results suggest that the effect of interglycosidic linkage of disaccharide attached to threonine on the antibacterial activity is more pronounced than the nature of distal sugar of glycosylated analogs of these proline-rich AMPs. Different configuration of interglycosidic linkages (α or β) are known to influence the *N*-glycosidic torsion angle at different extents [25] in case of *N*-linked glycosides. It has been reported that small changes in carbohydrate composition are sufficient to induce conformational changes in the peptide [26]. Hence, the variation in the antibacterial activity of these disaccharide-bearing analogs may be due to the difference in the nature of distal sugar and/or interglycosidic linkage between two sugars, which in turn may affect the conformation of the peptide and resulting differences in their binding affinity for target molecules.

Kinetics of DnaK-Peptide Interactions

Proline-rich AMPs have been reported to bind the substrate binding domain of bacterial heat-shock protein and DnaK and inhibit its function [14]. To determine whether differential–antibacterial pattern of these analogs resulted from different binding affinities of these peptides to substrate binding domain of DnaK, we have studied the comparative binding interactions of the synthesized peptides to DnaK. Interestingly, all the glycosylated analogs of formaecin I and drosocin showed comparable dissociation constants (K_D) in micromolar range (Table 2). β-D-maltosyl-formaecin I and β-D-maltosyl-drosocin displayed the highest antibacterial activity among the other synthesized analogs of the corresponding peptides, but all these peptides exhibited similar binding affinity to DnaK. Recent investigations have revealed that a proline-rich AMP, apidaecin analog Api88 and its two truncated versions were equally efficient in binding to DnaK, but only the full length Api88 was active [27]. In our earlier studies, we have also demonstrated that both D and L enantiomers of drosocin analog could bind to DnaK with similar affinity but only L enantiomeric form of the peptide displayed the antibacterial activity [22].

Thus, the aforementioned results showing similar binding affinity to DnaK for differentially glycosylated analogs of formaecin I and drosocin cannot explain the differences in their antibacterial activity. Hence, we further analyzed this issue by studying the internalization of these peptides into bacterial cells using flow cytometry.

Bacterial Uptake of FITC-Labeled Peptides

To rationalize the higher antibacterial potential of β-D-maltosyl-formaecin I and β-D-maltosyl-drosocin and its correlation with their uptake into bacterial cells, we synthesized FITC-labeled formaecin I and drosocin analogs carrying β-glucosyl and β-maltosyl (Table 1). The cellular internalization of these labeled glycopeptides was then examined by flow cytometry. Figure 3 displayed the bacterial uptake of peptides. Around 5% and 36% of the *E. coli* ATCC25922 cells were observed to be FITC-positive within 30 min when treated with FITC-β-D-glucosylated and FITC-β-D-maltosylated formaecin I, respectively, and the percentage of fluorescent cell population increased in 60 min to around 6% and 54%, respectively (Figure 3A). β-D-maltosyl-formaecin I was three times more potent than β-glucosyl formaecin I for *E. coli* ATCC25922 and internalized much faster and stained around seven times more number of cells than that of β-D-glucosyl-formaecin I. When bacterial cells were incubated with FITC-labeled drosocin analogs containing β-D-glucosyl and β-D-maltosyl, approximately 18% and 37% of the cells after 30 min and around 38% and 62% of the cellular population at 60 min, respectively, were observed to be FITC-positive (Figure 3B). The antibacterial activity of β-D-maltosyl-drosocin was observed to be around 1.5 times more than that of β-D-glucosyl-drosocin that correlates with its two times higher number of cells staining in comparison with that of β-D-glucosyl-drosocin. Insignificant cell population was observed to be positive for PI, indicating no cell death in the samples.

The bacterial uptake studies by FACS experiments showed the correlation between the antibacterial activity of the glycopeptides and their internalization into the bacterial cells. Antibacterial

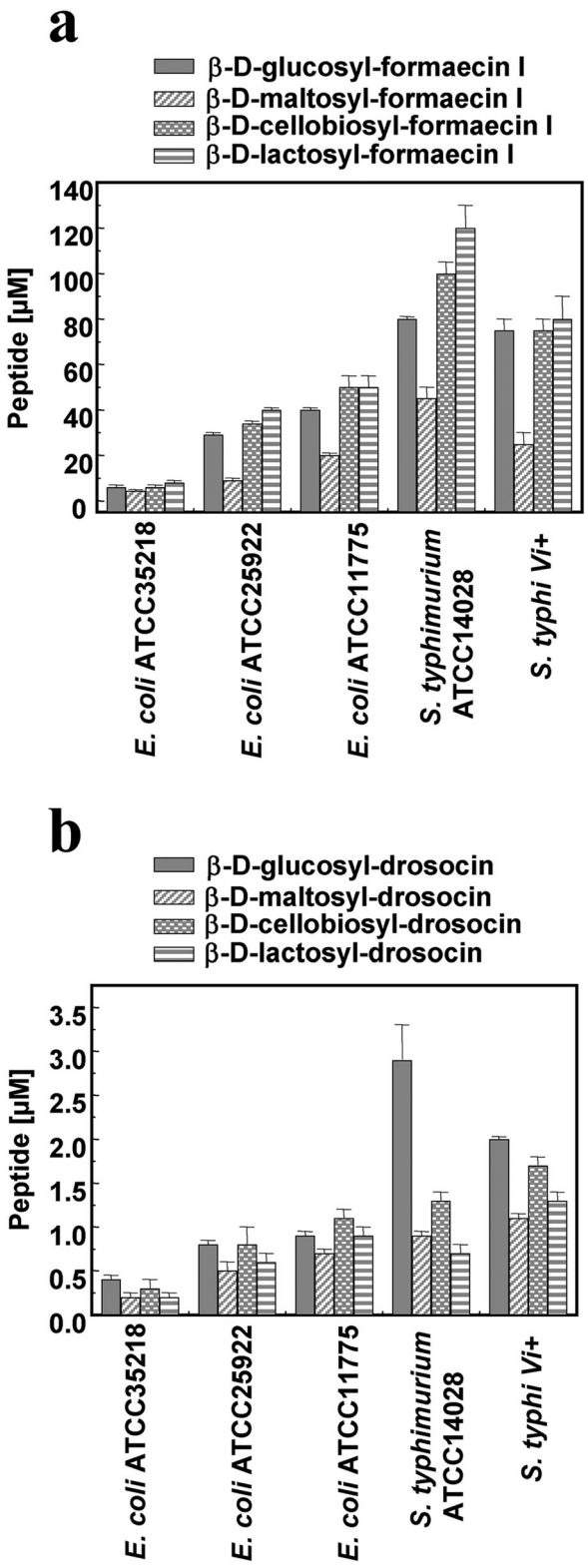

Figure 2. MICs of peptide analogs against various Gram-negative bacterial strains. A bar graph depicting MIC (μM) on *Y*-axis and bacterial strains, *E. coli* ATCC 35218, *E. coli* ATCC 25922, *E. coli* ATCC 11775, *S. typhimurium* ATCC 14028 and *S. typhi* Vi+ on *X*-axis for (a) *β*-D-glucosyl-formaecin I, *β*-D-maltosyl-formaecin I, *β*-D-cellobiosyl-formaecin I and *β*-D-lactosyl-formaecin I and (b) *β*-D-glucosyl-drosocin, *β*-D-maltosyl-drosocin, *β*-D-cellobiosyl-drosocin and *β*-D-lactosyl-drosocin. *β*-D-maltosyl-formaecin I and *β*-D-maltosyl-drosocin exhibited lowest MIC, thus highest activity against all the studied bacterial strains. The results represent the mean ± SEM of at least three independent experiments performed in triplicate.

Table 2. Kinetic parameters of interaction of formaecin I and drosocin analogs with Substrate Binding Domain (SBD)-DnaK (*E. coli*) at 25 °C

Peptide	k_{ass} (M^{-1}/s^{-1})	k_{diss} (s^{-1})	K_D (M)
β-D-glucosyl-formaecin I	1.66×10^4	0.0321	1.93×10^{-6}
β-D-maltosyl-formaecin I	1.89×10^4	0.0356	1.88×10^{-6}
β-D-cellobiosyl-formaecin I	2.13×10^4	0.0419	1.96×10^{-6}
β-D-lactosyl-formaecin I	2.66×10^4	0.0495	1.85×10^{-6}
β-D-glucosyl-drosocin	1.69×10^4	0.0450	2.67×10^{-6}
β-D-maltosyl-drosocin	1.60×10^4	0.0326	2.04×10^{-6}
β-D-cellobiosyl-drosocin	2.44×10^4	0.0266	1.09×10^{-6}
β-D-lactosyl-drosocin	2.17×10^4	0.0391	1.80×10^{-6}

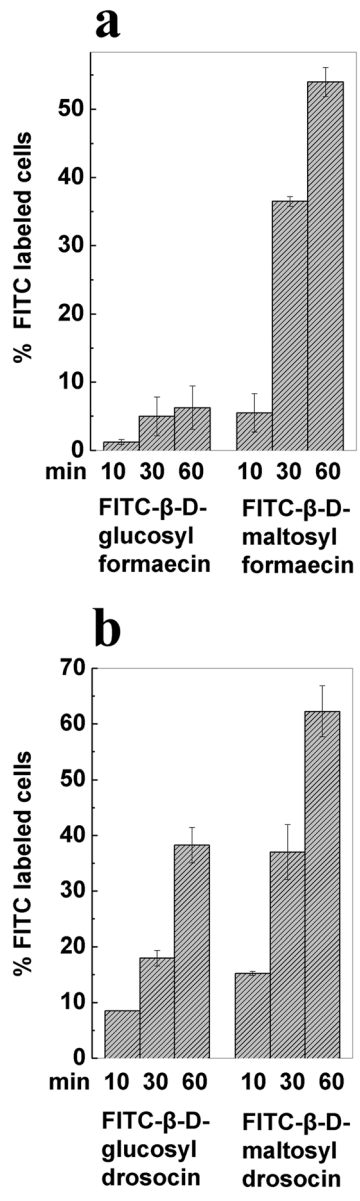

Figure 3. Fluorescence-activated cell sorting assay for measuring bacterial uptake of FITC-labeled peptides. *E. coli* ATCC25922 cells were incubated with (a) 10 μM of FITC-*β*-D-glucosyl-formaecin I and FITC-*β*-D-maltosyl-formaecin I (b) 4 μM of FITC-*β*-D-glucosyl-drosocin and FITC-*β*-D-maltosyl-drosocin for 10, 30 and 60 min. The results represent the mean ± SEM of at least three independent experiments.

Journal of PeptideScience

peptide possessing higher activity was internalized faster and stained higher percentage of bacterial cells in comparison with less-active antibacterial peptide. Thus, the higher antibacterial activity of β-D-maltosyl containing analogs of formaecin I and drosocin might be due to their faster internalization into the bacterial cells.

CD Studies

The comparative CD spectral analysis was carried out to measure the structural effects of monosaccharide and disaccharides on formaecin I and drosocin backbone in different solvents like PB (10 mM, pH7.4), 90% TFE/water and 10 mM SDS (Figures 4 and 5). The CD spectra of glycosylated analogs of formaecin I and drosocin in PB are shown in Figures 4A and 5A, respectively. The overall spectral profiles for all the glycosylated analogs of formaecin I and drosocin were similar, whereas the absolute values of the molar ellipticities varied among the analogs. The CD spectra of all the glycopeptides displayed random secondary structure in PB, with a strong negative band at around 200 nm. In 90% TFE/water and 10 mM SDS, all the glycopeptides exhibited spectral alterations as shown by the deviation in the curves to a more positive ellipticity (Figures 4B, 4C and 5B, 5C). All glycosylated analogs of formaecin I showed red shiftt of the negative band at 204 nm in TFE as well as SDS environment in comparison with that of spectra in 10 mM PB. The glycosylated analogs of drosocin did not exhibit such red shifts in presence of TFE or SDS. All glycosylated analogs of formaecin I and drosocin were unable to acquire the properly ordered secondary structure in 90% TFE/water as well as 10 mM SDS. Even in the presence of LPS, they predominantly showed the disordered conformation (Figure S1, Supporting Information). The CD spectra of all glycopeptides indicated absence of any regular secondary structure and displayed similar spectral characteristics.

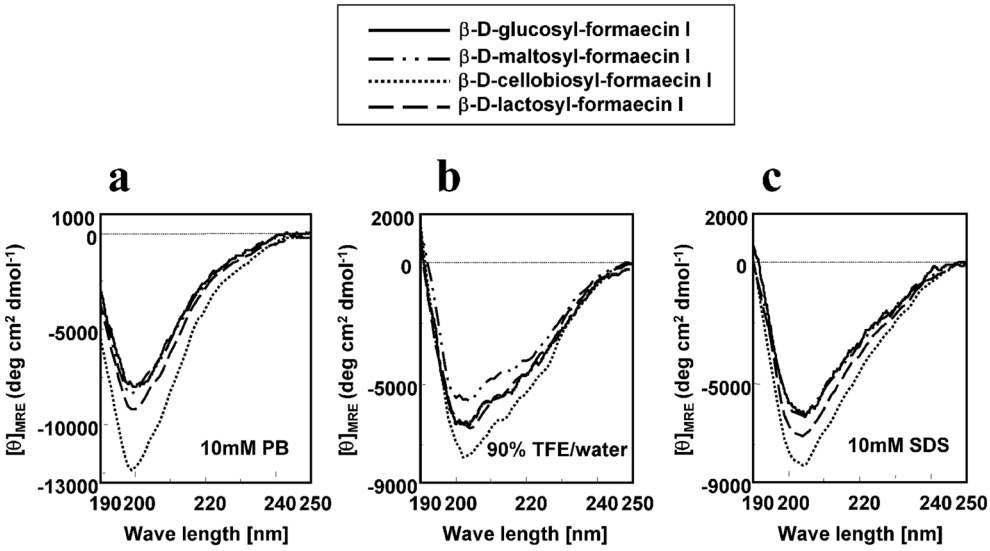

Figure 4. The secondary structures of formaecin analogs possess characteristics of random coil in different environments, and spectra are unaltered with change in the chain length of sugar. Circular dichroism spectra of β-D-glucosyl-formaecin I, β-D-maltosyl-formaecin I, β-D-cellobiosyl-formaecin I and β-D-lactosyl-formaecin I in (a) 10 mM PB pH 7.4 (b) 90% TFE/water (c) 10 mM SDS.

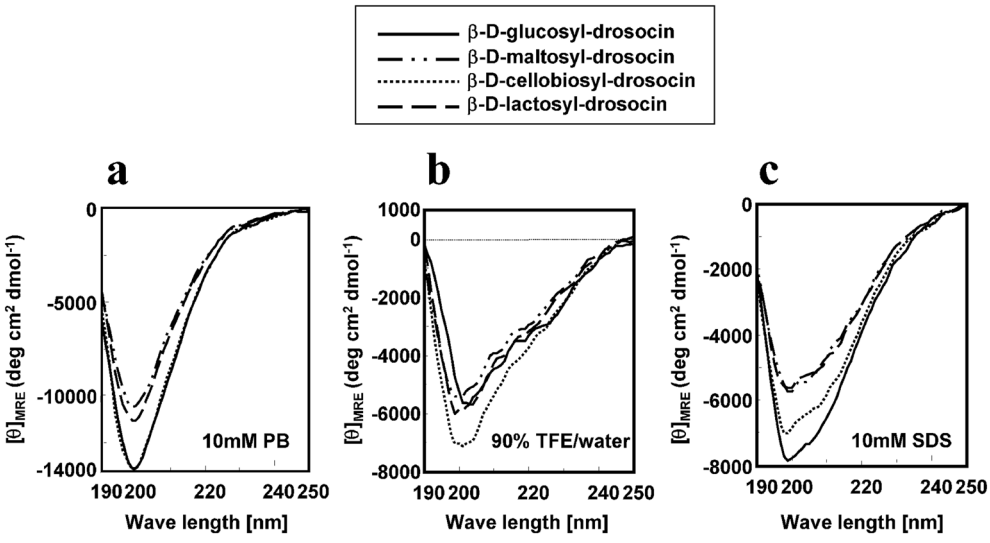

Figure 5. The secondary structures of drosocin analogs possess characteristics of random coil in different environments. Circular dichroism spectra of β-D-glucosyl-drosocin, β-D-maltosyl-drosocin, β-D-cellobiosyl-drosocin and β-D-lactosyl-drosocin in (a) 10 mM PB pH 7.4 (b) 90% TFE/water (c) 10 mM SDS.

Thus, CD studies of disaccharide analogs of formaecin I and drosocin displayed no significant variation due to change in the nature and glycosidic linkage of distal sugar. Their secondary structures were minimally affected by increase in sugar chain length as their CD spectra were similar to that of monoglycosylated counterpart, β-D-glucosyl-peptide. Moreover, in the earlier studies, it has been shown that the size of the sugar side chain did not play any role in defining the secondary structure of peptide [28]. The CD spectra of all the glycopeptides indicated the absence of any regular secondary structure, and their conformational properties in all the environments remained unaffected. We need high-resolution conformational analyses of these disaccharides containing glycopeptides to understand the detailed effect of these variations.

Cytotoxic Activity

To investigate the cytotoxicity of these disaccharides containing antimicrobial peptides on eukaryotic cells, the hemolytic activity

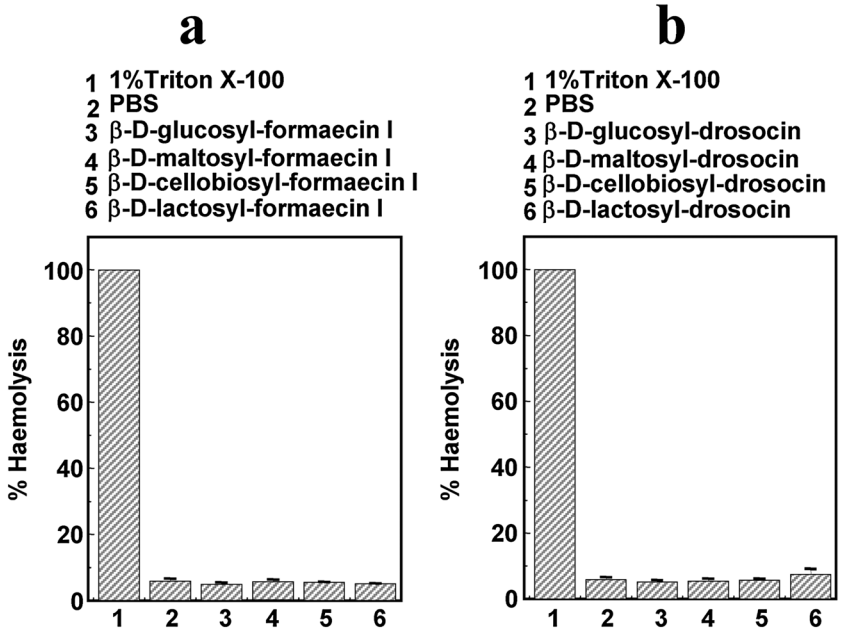

Figure 6. Hemolytic potential of differentially glycosylated formaecin I and drosocin analogs. Percentage hemolytic activity (*Y*-axis) is calculated after exposure of rat erythrocytes to 200 μM of (a) β-D-glucosyl-formaecin I, β-D-maltosyl-formaecin I, β-D-cellobiosyl-formaecin I, β-D-lactosyl-formaecin I and (b) β-D-glucosyl-drosocin, β-D-maltosyl-drosocin, β-D-cellobiosyl-drosocin and β-D-lactosyl-drosocin. Cells incubated with 10 mM PBS alone served as the negative control, and cells lysed using 1% Triton X-100 were used to measure 100% lysis (positive control). The results represent the mean ± SEM of at least three independent experiments performed in triplicate.

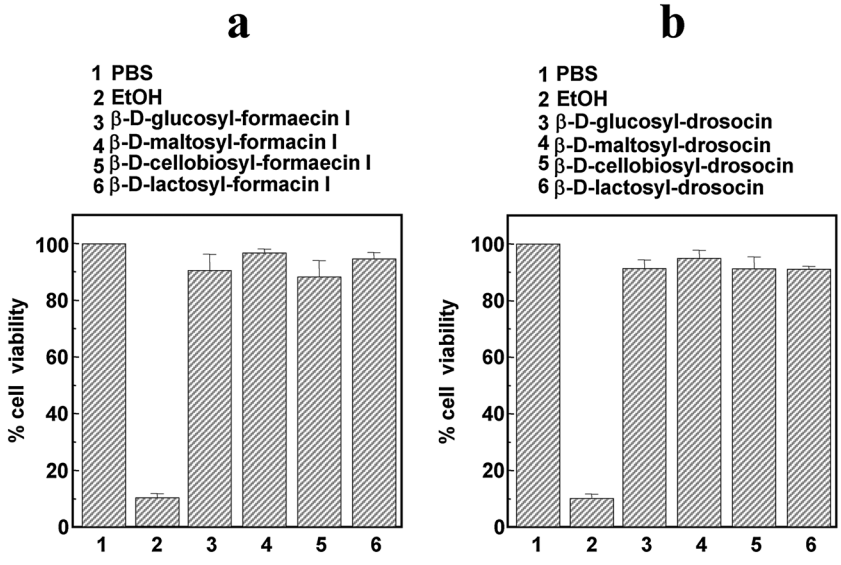

Figure 7. Cytotoxic potential of peptide analogs on macrophage cell line, J774**.** Percentage of cell viability (*Y*-axis) for murine macrophages cell line, J774 was calculated for (a) β-D-glucosyl-formaecin I, β-D-maltosyl-formaecin I, β-D-cellobiosyl-formaecin I, β-D-lactosyl-formaecin I and (b) β-D-glucosyl-drosocin, β-D-maltosyl-drosocin, β-D-cellobiosyl-drosocin and β-D-lactosyl-drosocin by standard MTT assay. Concentrations of peptides used are 1 mg/ml. In the positive and negative controls, the peptide was substituted with the same volume of ethanol and PBS, respectively. The results represent the mean ± SEM of at least three independent experiments performed in triplicate.

Journal of PeptideScience

and MTT assays were carried out. The effects of maltose, cellobiose and lactose containing formaecin I and drosocin on murine erythrocytes and J774 macrophage cell lines were evaluated and compared with that of their respective β-D-glucosylated analogs.

All the disaccharide containing analogs of formaecin I and drosocin showed less than 5% hemolytic activity at the concentration of 200 μM, when tested on 2% (vol/vol) suspensions of rat erythrocytes. All these peptides were non-toxic to rat blood cells. Similar results were obtained with their respective monoglycosylated β-D-glucosylated analogs when tested for their hemolytic activities on rat erythrocytes at the concentration of 200 μM. Thus, increasing the length of sugar chain does not affect the hemolytic activity of these peptides, and the disaccharides containing analogs of formaecin I and drosocin behave similar to the monoglycosylated forms (Figure 6A and 6B).

The cytotoxic potential of all the disaccharide containing peptides was also compared with that of monoglycosylated peptide by following incubation of exponentially growing murine macrophages cell line, J774 for 24 h with these peptides using MTT assay. All the tested peptides caused less than 10% of decrease in cell viability in comparison with that of control group with the concentration of 1 mg/ml. Thus, all the disaccharide containing antibacterial peptides did not show cytotoxicity on J774 cells similar to that of respective β-D-glucosylated analogs, in the present study (Figure 7A and 7B).

Conclusion

We have synthesized maltose, cellobiose and lactose containing analogs of formaecin I as well as drosocin that provide a model system to understand the effect of distal sugar and/or interglycosidic linkage on the lethal action of proline-rich class of AMPs. Lactose and cellobiose-bearing formaecin I analogs exhibited comparable antimicrobial activities. However, β-D-lactosyl-drosocin was marginally more potent than that of β-D-cellobiosyl-drosocin. Among the studied analogs, maltose containing formaecin I as well as drosocin showed highest activity. The magnitude of variation in antimicrobial activities among different analogs of formaecin I was not similar to that of drosocin analogs, probably due to difference in the polypeptide sequence around glycosylation site. All the synthesized glycosylated analogs of formaecin I and drosocin exhibited similar binding affinity to DnaK. Higher antibacterial activity of maltosyl containing peptides can be attributed to their higher rate of internalization into bacterial cells in comparison with that of other glycosylated analogs. Change in nature of interglycosidic linkage and/or distal sugar did not change secondary structures of peptide analogs as characterized by CD. Further, high-resolution conformational analyses would be required to evaluate the precise structural effect of a different disaccharide on these glycopeptides. Our findings demonstrate that sugar chain length may affect the antibacterial potential of proline-rich class of AMPs and even the nature of interglycosidic linkage of disaccharide may play an important role in affecting their function. Thus, proline-rich class of AMPs may be considered as a good example for investigating structure-function correlation studies of glycosylated peptides.

Acknowledgements

We thank the Department of Science and Technology (project no.: SR/S1/OC-63/2012), India, for the financial support. D. S. L. was a recipient of a senior research fellowship from the Council for Scientific and Industrial Research (CSIR), India. We also thank Ms. Archana Ranjan and Ms. Shanta Sen for the help with HRMS data.

References

1 Dwek RA. Biological importance of glycosylation. *Dev. Biol. Stand.* 1998; **96**: 43–47.
2 Parekh BR. Effects of glycosylation on protein function. *Curr. Opin. Struct. Biol.* 1991; **1**: 750–754.
3 Sola RJ, Griebenow K. Effects of glycosylation on the stability of protein pharmaceuticals. *J. Pharm. Sci.* 2009; **98**(4): 1223–1245.
4 Pratt MR, Bertozzi CR. Synthetic glycopeptides and glycoproteins as tools for biology. *Chem. Soc. Rev.* 2005; **34**: 58–68.
5 Liang R, Andreotti AM, Kahne D. Sensitivity of glycopeptides conformation to carbohydrate chain length. *J. Am. Chem. Soc.* 1995; **117**(41): 10395–10396.
6 Cudic M, Ertl HCJ, Otvos L, Jr. Synthesis, conformation and T-helper cell stimulation of an O-linked glycopeptides epitope containing extended carbohydrate side-chains. *Bioorg. Med. Chem.* 2002; **10**(12): 3859–70.
7 Shinohara H, Matsubayashi Y. Chemical synthesis of *Arabidopsis* CLV3 glycopeptide reveals the impact of hydroxyproline arabinosylation on peptide conformation and activity. *Plant Cell Physiol.* 2013; **54**(3): 369–74.
8 Hoffmann D, Florke H. A structural role for glycosylation: lessons from the hp model. *Folding Des.* 1998; **3**: 337–343.
9 Tagashira M, Hideki I, Yukihiro I, Masayuki H, Shinji T, Yasuhisa F, Kumiko Y-K, Shuji I, Kiichiro N, Toshihiro Y, Tadashi T, Kazunori T. Site dependent effect of O-glycosylation on the conformation and biological activity of calcitonin. *Biochemistry* 2001; **40**: 11090–11095.
10 Bulet P, Dimarcq JL, Hetru C, Lagueux M, Charlet M, Hegy G, Van Dorsselaer A, Hoffmann JA. A novel inducible antibacterial peptide of *Drosophila* carries an O-glycosylated substitution. *J. Biol. Chem.* 1993; **268**(20): 14893–14897.
11 Cociancich S, Dupont A, Hegy G, Lanot R, Holder F, Hetru C, Hoffmann JA, Bulet P. Novel inducible antibacterial peptide from hemipteran insect, the sap sucking bug *Pyrrhocoris apterus*. *Biochem. J.* 1994; **300**: 567–575.
12 Mackintosh JA, Veal DA, Beattie AJ, Gooley AA. Isolation from an ant *Myrmecia gulosa* of two inducible O-glycosylated proline rich antibacterial peptides. *J. Biol. Chem.* 1998; **273**(11): 6139–6143.
13 Castle M, Nazarian A, Yi SS, Tempst P. Lethal effects of apidaecin on *Escherichia coli* involve sequential molecular interactions with diverse targets. *J. Biol. Chem.* 1999; **274**(46): 32555–32564.
14 Otvos L, Jr, Insug O, Rogers ME, Consolvo PJ, Condie BA, Lovas S, Bulet P, Blaszczyk-Thurin M. Interaction between heat shock proteins and antimicrobial peptides. *Biochemistry* 2000; **39**(46): 4150–4159.
15 McManus AM, Otvos L, Jr, Hoffmann R, Craik DJ. Conformational studies by NMR of the antimicrobial peptide, drosocin, and its non-glycosylated derivative: effects of glycosylation on solution conformation. *Biochemistry* 1999; **38**(2): 705–714.
16 Bulet P, Hetru C, Dimarcq JL, Hoffmann D. Antimicrobial peptides in insects; structure and function. *Dev. Comp. Immunol.* 1999; **23**(4-5): 329–344.
17 Gobbo M, Biondi L, Filira F, Gennaro R, Benincasa M, Scolaro B, Rocchi R. Antimicrobial peptides: synthesis and antibacterial activity of linear and cyclic drosocin and apidaecin Ib analogues. *J. Med. Chem.* 2002; **45**(20): 4494–4504.
18 Talat S, Thiruvikraman M, Kumari S, Kaur KJ. Glycosylated analogues of formaecin I and drosocin exhibit differential pattern of antibacterial activity. *Glycoconj. J.* 2011; **28**(8-9): 537–555.
19 Chang CD, Meienhofer J. Solid-phase peptide synthesis using mild base cleavage of N alpha-fluorenylmethyloxycarbonylamino acids, exemplified by a synthesis of dihydrosomatostatin. *Int. J. Pept. Protein Res.* 1972; **11**(3): 246–249.
20 Lele DS, Talat S, Kaur KJ. The presence of arginine in the Pro-Arg-Pro motif augments the lethality of proline rich antimicrobial peptides of insect source. *Int. J. Pept. Res. Ther.* 2013; **19**(4): 323–330.
21 Kimple AJ, Muller RE, Siderovski DP, Willard FS. A capture coupling method for the covalent immobilization of hexahistidine tagged proteins for surface plasmon resonance. *Methods Mol. Biol.* 2010; **627**: 91–100.
22 Lele DS, Talat S, Kumari S, Srivastava N, Kaur KJ. Understanding the importance of glycosylated threonine and stereospecific action of drosocin, a proline rich antimicrobial peptide. *Eur. J. Med. Chem.* 2015; **92**: 637–647.
23 Ren T, Liu D. Synthesis of targetable cationic amphiphiles. *Tetrahedron Lett.* 1999; **40**: 7621–7625.
24 Knorr R, Trzeciak A, Bannwarth W, Gillessen D. New coupling reagents in peptide chemistry. *Tetrahedron Lett.* 1989; **30**(15): 1927–1930.
25 Mathiselvam M, Ramkumar V, Loganathan D, Pérez S. Effect of distal sugars and interglycosidic linkage on the N-glycoprotein linkage

region conformation: synthesis and x-ray crystallographic investigation of β-1-N-alkanamide derivatives of cellobiose and maltose as disaccharide analogues of the conserved chitobiosylasparagine linkage. *Glycoconj. J.* 2014; **31**(1): 71–87.
26 O'Connor SE, Imperiali B. A molecular basis for glycosylation induced conformational switching. *Chem. Biol.* 1998; **6**(8): 427–437.
27 Berthold N, Hoffmann R. Cellular uptake of apidaecin 1b and related analogs in gram-negative bacteria reveals novel antibacterial mechanism for proline rich antimicrobial peptides. *Protein Pept. Lett.* 2014; **21**: 391–398.
28 Otvas L, Jr, Cudic M. Conformation of glycopeptides. *Mini Rev. Med. Chem.* 2003; **3**(7): 703–711.

Supporting Information

Additional supporting information may be found in the online version of this article at the publisher's web site.